CIMAC CONGRESS 25
ZURICH, MAY 19 – 23, 2025

2025 | 191

Efficiency and emissions of NH3-diesel/bio-pilot dual-fuel combustion in a high-speed four-stroke engine

Fuels - Alternative & New Fuels

Brian Kaul, Oak Ridge National Laboratory

Daanish Tyrewala, Oak Ridge National Laboratory
Scott Curran, Oak Ridge National Laboratory

ABSTRACT

While dual-fuel ammonia engines are starting to be commercialized for the large low-speed two-stroke marine engine market, there are still challenges with utilizing ammonia on four-stroke engines used as auxiliary engines for ocean-going vessels and in inland and coastal marine applications. The shorter timescales for high-speed engines pose a particular challenge for low-cetane, high ignition energy fuels like ammonia. In addition to achieving maximum ammonia substitution levels, N2O emissions are a key factor that needs to be understood. This paper reports the results of experiments using a single-cylinder 107mm bore Cummins B-series diesel engine modified for port-fuel injection of gaseous anhydrous ammonia with a direct injection of diesel fuel near-TDC to ignite the premixed ammonia. Combustion data as well as emissions data from an FTIR including NO, NO2, N2O, and unburned ammonia are presented for selected operating points with a focus on high-load operation at 1200rpm with high ammonia energy substitution (over 95% by fuel energy). Several air/fuel ratio conditions are included, sweeping from diesel-like airflow to stoichiometric conditions. The impact of biofuels (biodiesel and renewable diesel) as pilot fuels is also considered. Comparisons for emissions, greenhouse gas performance, and efficiency are made with a conventional diesel combustion baseline. The impact of fuel injection strategy on NOx, N2O, and NH3 emissions is quantified, and the dual-fuel ammonia results on this high-speed four-stroke engine are expected to provide fundamental insights into further combustion development opportunities for the larger engines used across marine applications.

1 INTRODUCTION

Ammonia is gaining broad interest as a chemical energy carrier for a variety of sectors as a vector for decarbonizing the economy [1]. In particular, ammonia is appealing as a zero-carbon fuel for marine transportation, where high power and long distance requirements necessitate the use of net-zero-carbon liquid fuels to meet greenhouse gas (GHG) reduction targets such as those set by the International Maritime Organization (IMO) [2]. While there are toxicity concerns with ammonia, there is significant infrastructure and process knowledge that can be leveraged due to its widespread use as a fertilizer making it one of the most commonly produced and shipped chemicals globally, with significant handling infrastructure at ports. There are several technical challenges to be solved surrounding its use as a fuel, including unfavorable combustion properties (e.g. low flame speed, high ignition energy) and high NO_x emissions [3]. Emissions of N_2O are also of particular concern due to its high global warming potential (GWP) [4], which could offset the reductions in CO_2 emissions gained from using ammonia.

Major marine engine companies including MAN E.S. [5], WinGD [6], and Wärtsilä [7] are currently developing ammonia-fueled marine engines for commercial availability. Combustion and emissions in ammonia-fueled engines are also a current research focus for academic and independent research laboratories.

An experimental investigation of ammonia dual-fuel combustion in a high-speed four-stroke engine with premixed ammonia and direct injection of diesel fuel by Wermuth *et al.* [8] revealed that low levels of emissions can be obtained from diesel/ammonia combustion using greater than 80% (by energy) ammonia and excess air ratio of less than 1.4. The authors also suggested the need for crevice volume reduction to facilitate the combustion of port-fueled ammonia and reduce N_2O emissions.

Auer *et al.* [9] examined dual-fuel operation with high-pressure direct injection of liquid ammonia rather than a premixed ammonia/air charge. Relative to the diesel baseline, an improvement in NO_x emissions was observed at the expense of considerable unburned ammonia. However, a significant reduction in engine-out N_2O and NH_3 emissions was reported at medium engine speeds compared to high-speed dual-fuel operation.

Schlick *et al.* [10] used a premixed ammonia approach similar to Wermuth *et al.* [8], albeit on a medium-speed single-cylinder engine. The authors emphasized the need for developing aftertreatment solutions for unburned ammonia and N_2O for such applications. They demonstrated zero tailpipe NH_3 emissions for low to high diesel replacement (10-70% NH_3 by energy), while underscoring the importance of high exhaust temperatures (>500°C) for successful N_2O conversion over a ruthenium catalyst. Ammonia/hydrogen blends were also discussed as a potential avenue for NH_3 and N_2O reduction.

Niki *et al.* [11] conducted experiments on a small-bore single-cylinder 4-stroke engine using a diesel pilot to ignite a premixed charge of either NH_3/air or NH_3/hydrogen/air. Although the results were not optimized, an improvement in N_2O and NH_3 was noted with the inclusion of hydrogen at the expense of higher NO_x compared to NH_3/air operation.

Recent work by Kurien and Rousselle [12] delved into the effects of NH_3 equivalence ratio on N_2O emissions in an engine capable of spark-ignition (SI) and compression-ignition (CI) operation in a diesel-pilot dual-fuel configuration. Their results, collected with elevated intake temperatures, indicated negligible N_2O emissions at lean conditions for both SI and CI operation, and at stoichiometric conditions for SI combustion, with richer operation being needed before N_2O emissions were observed relative to the CI combustion mode.

Several hypotheses have been posited to explain the processes underlying the N_2O emissions observed in NH_3-fueled engines. Jespersen *et al.* [13] attributed the formation of N_2O to the partial post-oxidation of the crevice-outgassed NH_3 during the expansion stroke in their SI experiments. Northrop [14], from his 0D modeling efforts, suggested that N_2O formation occurs over a wide range of equivalence ratios at low temperature regions where significant unburned NH_3 is available. However, it is reduced to low levels during the expansion stroke after an initial increase due to the thermal de-NO_x mechanism, indicating that quenching near cold surfaces is likely the primary driver of N_2O emissions for premixed NH_3 combustion.

While diesel/ammonia combustion can result in significantly lower GHG emissions compared to diesel-only operation, reaching a net-zero target will require the displacement of petroleum in the pilot fuels as well. For dual-fuel ammonia strategies, the use of a biofuel as the pilot fuel (bio-pilots) offers an attractive alternative to petroleum-derived fuel oils [15,16]. Bio-pilots have been used in other dual-fuel combustion approaches both for reduction of GHG and to take advantage of chemical and physical property differences compared to fossil-derived diesel fuels [17]. Biodiesel and renewable diesel have previously been used to improve dual-fuel reactivity-controlled compression-ignition combustion with fuels other than ammonia [18,19], specifically to take advantage of the high cetane number for renewable diesel and the oxygen content for biodiesel. Several studies have previously demonstrated the feasibility of ammonia/biodiesel dual-fuel combustion [20,21], though they have not compared the performance and emissions to ammonia dual-fuel combustion with other pilot fuels.

Both biodiesel and renewable diesel also serve as drop-in solutions suitable for operation in existing diesel engines, while retaining operational fallback flexibility in cases where ports do not have NH_3 available for bunkering. Xu *et al.* [22] report lifecycle GHG reductions of 40–69% for biodiesel and renewable diesel fuels produced from oil seed crops including soybean, canola, and carinata oil feedstocks (including land-use change estimations) and 79–86% for tallow, used cooking oil, and distillers corn oil feedstocks. To evaluate the lifecycle GHG impact of the biofuels used in this study, values of 67% GHG reduction for biodiesel (soy biodiesel including land use change) and 83% GHG reduction for renewable diesel (tallow/used cooking oil) compared to petroleum-based diesel were used.

While bio-pilot fuels offer a path to offset the CO_2 emissions from the pilot fuel on a well-to-wake basis, N_2O emissions remain a concern. Two approaches could then be used to reach true net-zero lifecycle GHG emissions for NH_3 dual-fuel engines. The first is to reduce the N_2O emissions through engine calibration (operation at richer conditions reduces engine-out N_2O emissions from incomplete NH_3 combustion) and aftertreatment optimization (minimization of N_2O that may be formed over an SCR as well as dedicated catalysts to reduce N_2O in the exhaust). Catalytic solutions for N_2O reduction are also likely to play a role, as mentioned by Schlick *et al.* [10]. While N_2O is a very stable molecule that is generally difficult to reduce catalytically, recent studies do show some success, particularly in the presence of NH_3 [23]. The second, which could complement these efforts, would be to use bio-fuels with a net-negative GHG impact (e.g. HTL oils produced from waste feedstocks [15]) as pilot fuels to achieve net-zero well-to-wake emissions by offsetting the impact of any N_2O emissions that cannot be eliminated. The viability of this approach in practice will be dependent on regulatory frameworks and whether net-negative feedstock credits are accepted.

In this work, renewable diesel and biodiesel are investigated as bio-pilot fuels alongside petroleum-based diesel as pilot fuels for dual-fuel diesel/ammonia combustion on a high-speed four-stroke engine.

2 EXPERIMENTAL SETUP & METHODOLOGY

2.1 Experimental Setup

2.1.1 Engine Specifications

This work was conducted using a Cummins B-series four-stroke high-speed diesel engine that was modified to operate on a single cylinder by disabling five of the six cylinders. The combustion chamber and diesel fuel injection systems are unmodified from the production engine and feature a centrally mounted common rail diesel fuel injector and re-entrant bowl piston geometry. Table 1 shows detailed engine specifications.

Table 1. Engine specifications

Number of cylinders	1
Bore	107 mm
Stroke	124 mm
Connecting rod length	145.4 mm
Compression ratio	20:1
Displacement volume	1.115 l
Diesel fuel injector	CRIN-3, 8-hole, 140 µm, 145° included angle
Ammonia fuel injectors	Clean Air Power DigiJet NH3ICE SP-010 (x2)

The engine was supplied with pressurized air from an air compressor, and an electronically controlled exhaust backpressure valve was used to simulate a turbocharger. Further details of the test cell systems including air, exhaust, coolant, and oil conditioning can be found in Curran *et al.* [24]. The engine was controlled using an open LabVIEW-based engine control system

2.1.2 Ammonia Fuel System

An NH_3 port fuel injection system comprising two Clean Air Power [25] DigiJet NH3ICE SP-010 fuel injectors was added to enable dual-fuel NH_3-diesel operation. The NH_3 fuel injectors were installed

approximately 35 cm upstream of the intake port, in a “y-section” to allow for mixing with the intake air, as shown in Figure 1. Anhydrous NH_3 was sourced from industrial cylinders with liquid dip tubes, routed through a vaporizer that used hot engine-out coolant to boil the NH_3 and provide a gaseous NH_3 fuel supply to the injectors. Fuel lines between the vaporizer and injectors were heat traced to prevent condensation. The NH_3 fuel supply system was interlocked with both the test cell ventilation system and NH_3 gas monitors for leak detection to ensure safe operation.

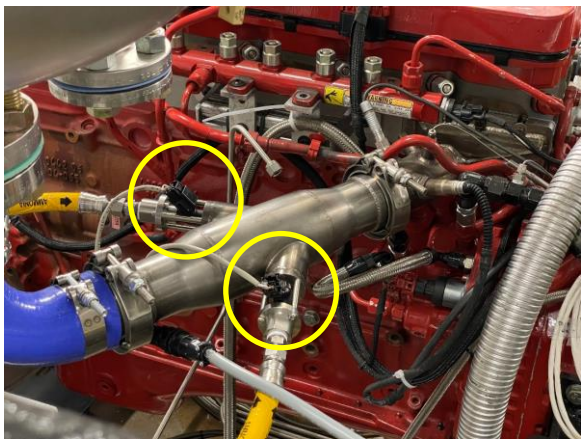

Figure 1. Ammonia fuel injectors (circled) installed on the single-cylinder engine

2.1.3 Instrumentation and Data Acquisition

An in-house LabVIEW-based code, Oak Ridge Combustion Analysis System (ORCAS), was integrated with the engine control system and used for data acquisition and real-time analysis. The engine was instrumented for in-cylinder pressure measurement using a Kistler model 6058A water-cooled pressure transducer, and cylinder pressure data were collected with 0.2°CA resolution, triggered using an AVL 365C shaft encoder. ORCAS was used to perform combustion analysis including heat release rate and combustion phasing during operation. Low-speed data (e.g. pressures, temperatures, air and fuel flow rates) were also collected and incorporated into the data files.

Engine exhaust gaseous emissions measurements were conducted using California Analytical Instruments (CAI) emissions O_2 (paramagnetic) and hydrocarbon (flame ionization detector) analyzers and a MKS Fourier Transform Infrared (FTIR) spectrometer. Particulate emissions were measured using an AVL Micro Soot Sensor. The FTIR was used to measure NO, NO_2, N_2O, NH_3, CO, CO_2, H_2O, and other species of interest. For this study, an FTIR method suitable for measurement of up to 15% NH_3 was used due to the potential for high engine-out unburned NH_3 emissions. Emissions calculations were performed using an open-source, LabVIEW-based emissions calculator by Dempsey and Ghandhi [26], which was integrated into the ORCAS data acquisition system and modified by adding additional calculations appropriate to NH_3 combustion, including NH_3 fuel energy substitution levels and N_2O GHG contributions.

2.2 Engine Operating Conditions and Fuels

The engine was operated at steady state conditions with high NH_3 energy substitution levels (90–96%) at 1200 rpm and approximately 12.6 bar net indicated mean effective pressure ($IMEP_n$). This represents a low-speed, medium-load condition on this engine, and is within the operating window where the engine can be operated well with high NH_3 energy substitution levels. The engine was initially operated with airflow maintained the same as for diesel operation, resulting in a λ of 1.6. Richer equivalence ratios (λ of 1.4 and 1.0) were also tested by reducing the air flow with a constant fuel energy input. For all cases, the exhaust backpressure was maintained at 15–20 kPa below the intake manifold pressure to simulate realistic turbocharger conditions. No exhaust gas recirculation was used in this study. For dual-fuel operation, a single diesel pilot injection close to TDC strategy was used. Diesel baseline comparison is to a two-injection (pilot + main) strategy. Details of engine operating conditions are shown in Table 2. Data were collected for 500 consecutive engine cycles and averaged for each operating condition.

Table 2. Engine operating conditions

Engine speed	1200 rpm
Engine load	~ 12.6 bar $IMEP_n$
Ammonia energy substitution	90–96%
Intake air temperature	60°C
Engine oil temperature	95°C
Engine coolant temperature	95°C
$P_{intake} - P_{exhaust}$	~ 15 kPa
λ	1, 1.4, 1.6
Diesel pilot SOI	λ = 1: 9°BTDC λ = 1.4, 1.6: 3°BTDC
Ammonia SOI	320°BTDC
Pilot fuels	ULSD, B100, RD

The experiments were repeated with three different pilot fuels: a certification grade ultra low sulfur diesel (ULSD)—Haltermann Solutions HF-00582 [27], 100% fatty acid methyl ester (FAME) biodiesel (B100), and renewable diesel (RD). The biodiesel and renewable diesel were sourced from Chevron Renewable Energy Group. Selected fuel properties are shown in Table 3.

Table 3. Fuel properties

Fuel	LHV (MJ/kg)	Density (kg/l)	Cetane Number
ULSD	42.2	0.8557	40.8
B100	37.3	0.8836	54.1
RD	43.8	0.7856	84.9
NH_3	18.8	0.6090	~ 0

3 RESULTS AND ANALYSIS

3.1 Fuel Efficiency and Thermodynamic Analysis

At the engine operating conditions examined in this study, the engine is operable at NH_3 energy substitution levels of over 95% with good performance and combustion stability for the ULSD baseline as well as both bio-pilot fuels, with indicated thermal efficiencies of 46–48% and COV of IMEP < 4% for all cases (and COV < 3% for $\lambda \leq 1.4$). Figures in this section show results with the ULSD pilot fuel only, for simplicity. Impacts of the bio-fuel pilots will be discussed in section 3.3. Due to the reduced energy density of NH_3 relative to diesel fuel, the indicated specific fuel consumption increases for NH_3 dual-fuel operation, as shown in Figure 2. However, the thermal efficiency is essentially unchanged relative to diesel baseline operation, as shown by the indicated work percentage in Figure 3.

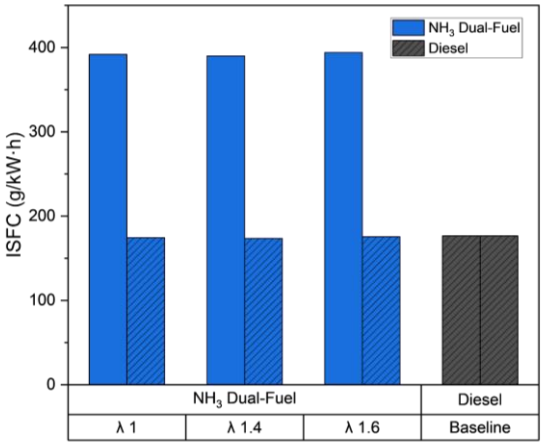

Figure 2. Indicated specific fuel consumption (ISFC) for NH_3 dual-fuel operation. Hashed bars for NH_3 dual-fuel cases are adjusted to diesel-equivalent values based on fuel LHV. Diesel baseline shown for reference.

While the net thermal efficiency is unchanged, the first-law thermodynamic balance shown in Figure 3 does have several interesting features. First, considering the "Other" category—which is the balance term and comprises primarily heat transfer (e.g. to coolant, oil, radiative/convective to the room, etc.), as well as any other unaccounted-for energy flux out of the system—it can be noted that there is a significant reduction in the overall losses here for the lean NH_3 dual-fuel cases relative to the diesel baseline. With current instrumentation on the engine, it is possible to calculate the heat rejection to the coolant, which is shown in Figure 4. It can be seen here that heat transfer to the engine coolant is significantly reduced for NH_3 dual-fuel operation, relative to the diesel baseline. A detailed explanation requires further exploration but may include factors such as reduced gamma, reduced impingement on the piston bowl by the diesel flame, lower adiabatic flame temperature and soot radiation, and other combustion-related impacts. Charge cooling is not a factor here, as the NH_3 was supplied to the engine in a vapor state. Heat transfer to the oil is not explicitly calculated, as the oil flow rate was not available, but the delta T across the engine for oil also reduces for ammonia dual-fuel combustion relative to the diesel baseline, indicating reduced heat transfer to the piston as well as the cylinder head.

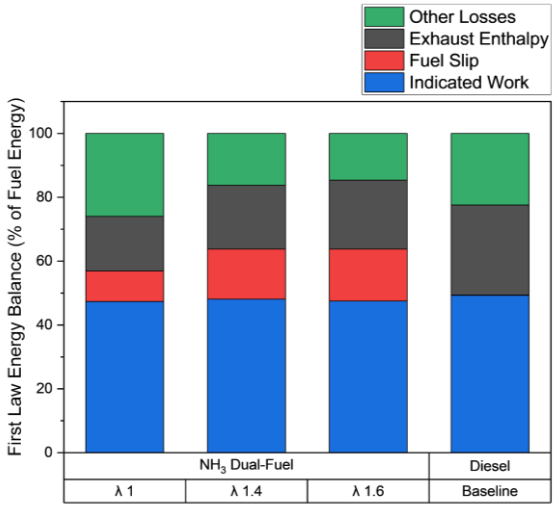

Figure 3. First law thermodynamic balance for NH_3 dual-fuel operation, compared to diesel baseline. Expressed in percentage of total fuel energy input.

A second notable feature in Figure 3 is that the NH_3 fuel slip (i.e., the unburned NH_3 in the engine-out exhaust) accounts for a significant fraction of the fuel energy for NH_3 dual-fuel combustion. Rather than a reduction in overall thermal efficiency, however, it is the heat transfer and exhaust enthalpy that make up a reduced share of the fuel energy input. The small reduction in exhaust enthalpy could at first glance have implications for turbocharging, but as noted in Tyrewala *et al*. [28] and shown in section 3.2 below, the optimal equivalence ratio for NH_3 dual fuel combustion—particularly when considering N-based emissions—is slightly richer than for diesel, with airflow requirements reduced accordingly. For the

fixed pressure differential across the engine used in these experiments, the calculated turbocharger efficiency was lower for all NH_3 dual-fuel equivalence ratios than for the diesel baseline condition, as shown in Figure 5.

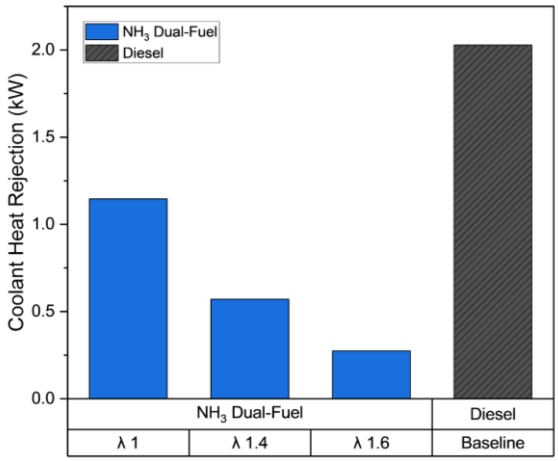

Figure 4. Coolant heat rejection for NH_3 dual-fuel operation, compared to diesel baseline.

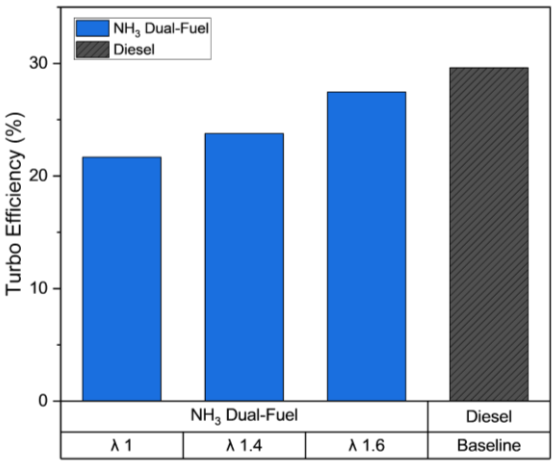

Figure 5. Turbocharger efficiency calculated for constant pressure ratio across engine with target airflow for NH_3 dual-fuel and diesel baseline operation.

Improved combustion chamber design (e.g. reduced crevice and squish volumes) and other features to reduce NH_3 slip could lead to improved efficiency, and some of the NH_3 present in the exhaust will also offset the need for additional dosing of NH_3 into SCR aftertreatment systems for NO_x reduction.

A final noteworthy feature of Figure 3 is that the NH_3 fuel energy slip is reduced at the stoichiometric case relative to lean conditions. However, this reduction is not resulting in an increase in indicated work, heat transfer, or exhaust enthalpy: rather, this shows up in the “other” category as energy that is not being accounted for by measurements with current instrumentation. It is possible that at this condition, some of the unburned NH_3 is reformed into other calorific species (e.g. hydrogen) that are not being measured, which could have implications for operating strategies including exhaust gas recirculation.

3.2 Engine-Out Emissions

The high NH_3 energy substitution level used in this study results in overall GHG reductions between 75 and 90%, as shown in Figure 6. Here, N_2O is accounted as having 273 times the GWP of CO_2 on a 100-year basis, per the IPCC Sixth Assessment Report [4].

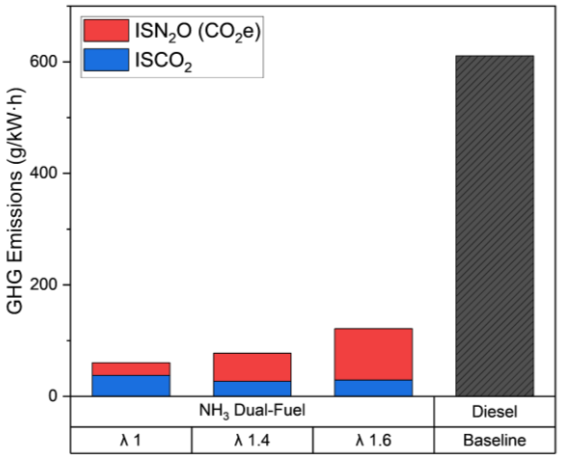

Figure 6. Greenhouse gas emissions (CO_2 and N_2O) from NH_3 dual-fuel operation, compared to diesel baseline CO_2 emissions. Expressed in net indicated specific CO_2-equivalent g/kw·h.

Engine-out criteria pollutant emissions are also of interest. Figure 7 shows emissions of unburned hydrocarbons (HC), CO, and NO_x. For all λ cases, the unburned hydrocarbon emissions increase by approximately a factor of two relative to the diesel baseline. Carbon monoxide emissions generally decrease for lean dual-fuel NH_3 combustion, but significantly increase at stoichiometric conditions. For lean conditions, where the exhaust conditions are similar to existing diesel aftertreatment systems, it may be possible to leverage existing emissions control technologies to eliminate the CO, HC, and NO_x emissions. Stoichiometric conditions, where the exhaust composition is substantially different, may require different approaches (e.g. two-way or three-way catalysis) to reducing NO_x and oxidizing HC, CO, and unburned NH_3.

NO_x emissions are also higher than the diesel baseline for lean dual-fuel operation with NH_3, peaking around a λ of 1.4 as previously reported [28], before dropping to levels below the diesel baseline for stoichiometric operation.

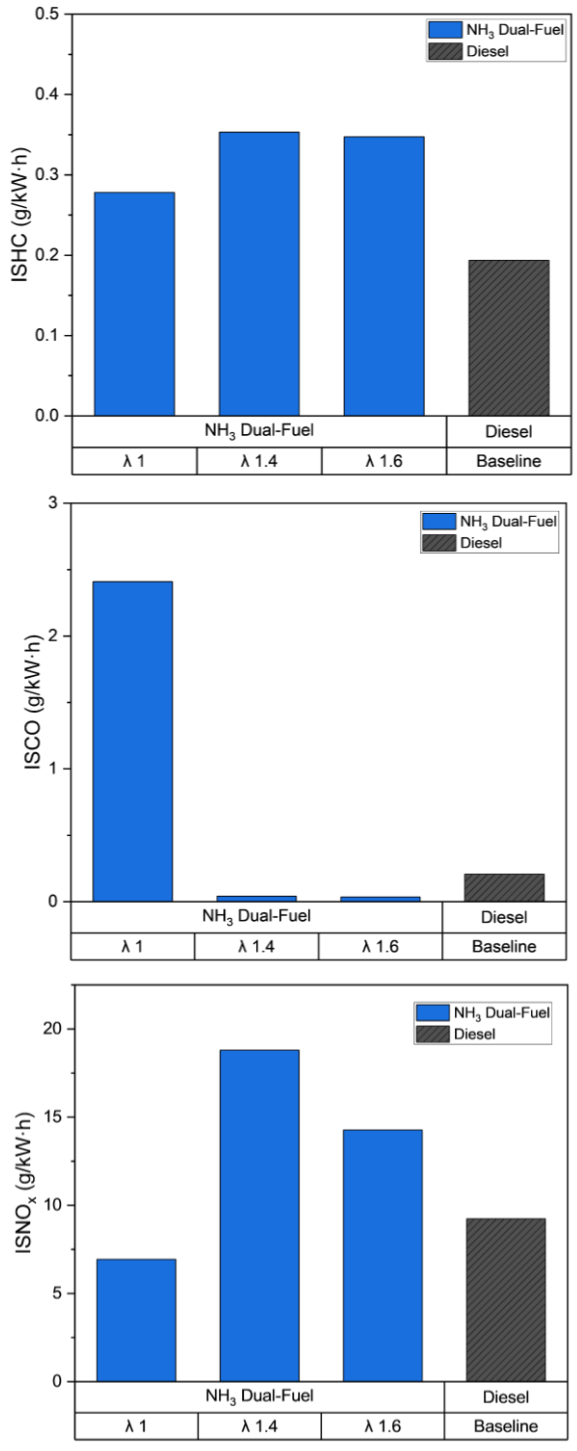

Figure 7. Indicated specific engine-out HC, CO, and NO_x emissions for NH_3 dual-fuel operation. Diesel baseline emissions also shown for reference.

Figure 8 shows bulk gas temperature calculated using the ideal gas law assuming constant composition for each case with the charge temperature at IVC pegged to the intake air temperature. The NO_x emissions observed in Figure 7 are not correlated with increased bulk gas T, which tends to confirm that the increased NO_x observed here for the lean NH_3 dual-fuel cases is primarily fuel-borne NO_x rather than thermal NO_x. As seen in Figure 9, there is also generally an inverse relationship between NH_3 slip and NO_x. This also points to NH_3 as the source of much of the NO_x, which is largely a product of incomplete combustion of NH_3.

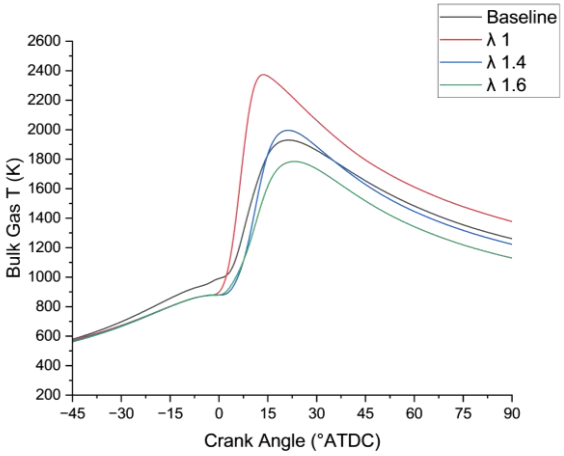

Figure 8. Bulk gas temperature for diesel baseline and NH_3 dual-fuel operation

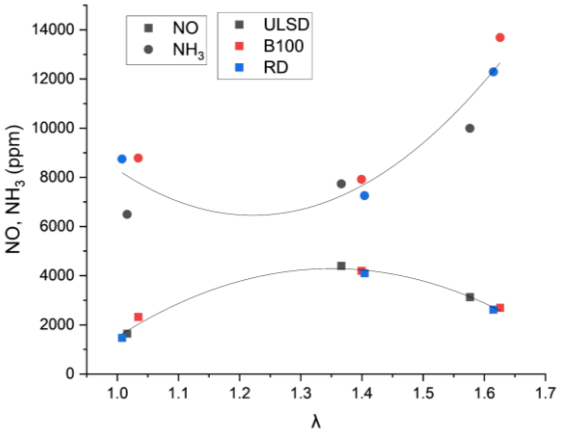

Figure 9. Engine-out NO_x and NH_3 emissions as a function of excess air ratio for all pilot fuels

The NO/NH_3 ratio is also relevant to mitigating the harmful NO_x and NH_3 emissions: selective catalytic reduction (SCR) aftertreatment systems utilize NH_3 to reduce NO_x, with an ideal molar ratio of 1:1. Due to non-idealities, a bit of extra NH_3 is generally needed to fully reduce the NO_x, but excessive NH_3 can also form N_2O in the SCR and should be avoided [29]. The presence of sufficient NH_3 in the exhaust to fully reduce the NO_x raises the possibility of using a passive SCR system (i.e. an SCR catalyst without a urea doping system that relies on engine-out NH_3 slip) to mitigate the emissions of both NH_3 and NO_x. Catalytic solutions to NH_3 slip and N_2O may help compliment such a passive SCR system. Optimization of an

engine/aftertreatment system to minimize harmful emissions will require balancing engine-out N_2O, NH_3, and NO_x emissions, efficiency, exhaust temperatures, and other factors.

Black carbon (BC), or soot, is another pollutant of concern in the marine sector. Ammonia dual-fuel operation in this engine was observed to reduce the emissions of BC relative to the diesel baseline for all equivalence ratios, as shown in Figure 10. While the emissions are reduced relative to the diesel baseline, the reduction is not proportional to the reduction in diesel fueling (~95%). Particulate mass concentration in this study was measured using an AVL Micro Soot Meter, which uses a photo-acoustic measurement technique which is primarily responsive to black carbon as opposed to organic carbon or ash. Additional investigation is needed to understand whether the particles being measured are entirely due to soot formed in the diesel pilot flame via conventional mechanisms or whether other generation pathways exist. For example, Patil *et al*. [30] hypothesized ammonium nitrate formation as a potential explanation for their observation of increasing particle number count with increasing NH_3 concentration in NH_3/H_2 SI combustion. Past studies have also shown some interaction between soot and ammonium nitrate particle species in catalysts [31]; it is conceivable that if these particles are present, they could be serving as nucleation sites for soot agglomeration. Oxidation of soot formed via conventional mechanisms could also be impeded by the reduced oxygen concentration in the late combustion period due to the premixed ammonia/air combustion.

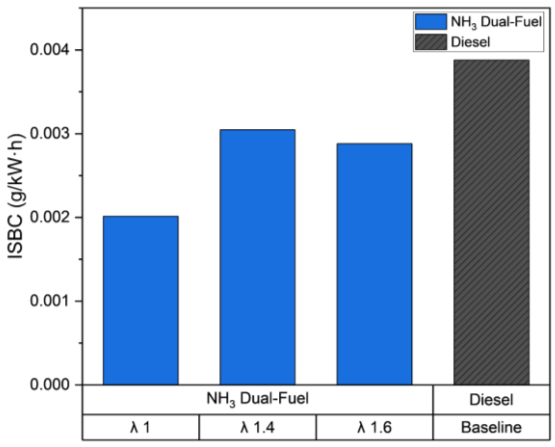

Figure 10. Engine-out indicated specific black carbon (ISBC) emissions for NH_3 dual-fuel operation. Diesel baseline emissions also shown for reference.

3.3 Impact of Bio-Pilot Fuels

The impact of bio-pilot fuels on the engine-out emissions for NH_3 dual-fuel combustion is also of interest. The primary motivation for the use of biofuels as pilot fuels is to take advantage of their low lifecycle carbon intensity and minimize GHG emissions relative to a petroleum-derived pilot fuel, in pursuit of net-zero GHG targets. Figure 11 shows the GHG emissions adjusted for lifecycle CO_2 impact of the biofuels for all pilot fuels. As can be seen here, applying these lifecycle carbon intensity factors to the $ISCO_2$ nearly eliminates the lifecycle GHG contributions from CO_2 but does not eliminate the contribution of the N_2O emissions. Use of net-negative GHG biofuels could offer a path to further offset these emissions.

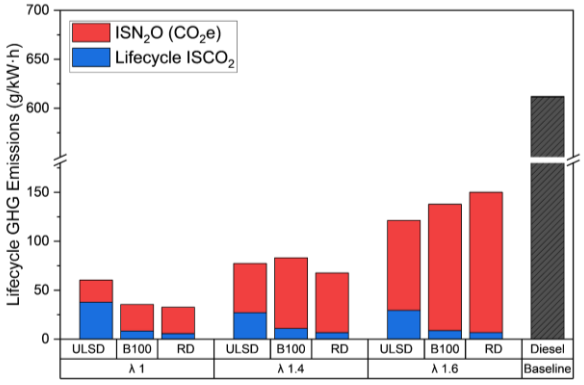

Figure 11. Greenhouse gas emissions (CO_2 and N_2O) from NH_3 dual-fuel operation, accounting for lifecycle carbon intensity of biodiesel and renewable diesel pilot fuels. Expressed in net indicated specific CO_2-equivalent g/kw·h. Diesel baseline CO_2 emissions also shown for reference (note broken vertical scale).

Initial observation of Figure 11 would appear to show a difference in the N_2O emissions contribution to GHG based on the pilot fuel, with slightly increased N_2O emissions for the bio-pilot fuels at lean operating conditions. However, as noted in Tyrewala *et al.* [28], there is a strong dependence of engine-out emissions on λ, with richer conditions favoring more complete combustion of the NH_3 and reducing N_2O emissions at the expense of increased NO_x. The differences in N_2O emissions that are seen in Figure 11 are actually caused by small offsets in the actual λ achieved in engine operation from the nominal target values, as can be seen in Figure 12. The choice of pilot fuel does not appear to have any real impact on N_2O emissions.

Unlike the gaseous emissions, there is a detectable impact of the pilot fuel on BC emissions, with the biofuels exhibiting reduced BC relative to the petroleum-based diesel fuel at all equivalence ratios, as shown in Figure 13. The biodiesel yielded the lowest soot emissions, likely due in large part to the 11% oxygen content of the fuel in addition to the lack of polyaromatic hydrocarbons (PAH) that typically serve as soot precursors in diesel combustion. The renewable diesel also reduced

BC emissions relative to the ULSD. This also has roots in the fuel composition: renewable diesel fuel is highly paraffinic [32], also lacking the PAH that are found in petroleum diesel fuels. The impact of the pilot fuel properties on the BC emissions indicates that the majority of the particulates being measured here are likely formed in traditional diesel soot formation pathways.

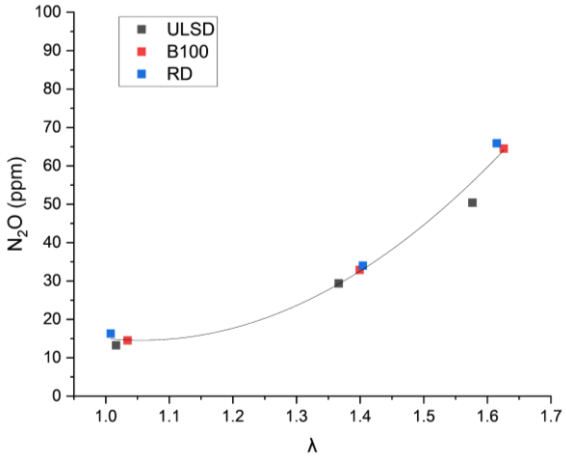

Figure 12. Engine-out N_2O emissions as a function of excess air ratio for all pilot fuels

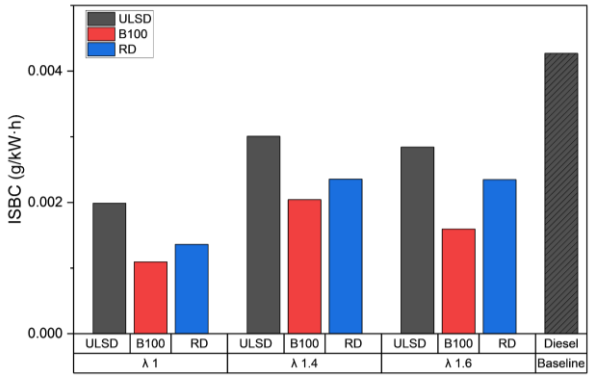

Figure 13. Engine-out black carbon emissions for NH_3 dual-fuel combustion with all pilot fuels. Diesel baseline emissions also shown for reference.

In addition to emissions, the pilot fuel properties also have some impact on combustion phasing. As shown in Figure 14, for the richer conditions, both bio-pilot fuels resulted in more advanced combustion phasing relative to the ULSD pilot fuel.

This is most apparent in the ignition delay period, here defined as the elapsed time between the commanded start of injection and CA05. Figure 15 shows that the ignition delay is in all cases shortest for the renewable diesel fuel and longest for the ULSD. This relationship is consistent with the cetane numbers of the fuels, shown in Table 3. The greatest impact is at the stoichiometric condition, where there is little excess air available and the SOI is earlier, which result in the least favorable conditions for ignition of the diesel pilot. While these conditions exhibited stable dual-fuel NH_3 combustion, it is possible that higher-cetane fuels like renewable diesel could expand the range of dual-fuel operation at other operating conditions, e.g. to earlier injection timings at low-load conditions. Further studies would be needed to quantify any potential benefit in practice.

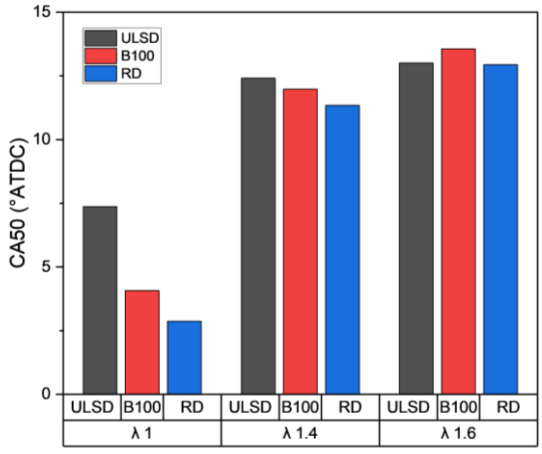

Figure 14. Combustion phasing (CA50) for all pilot fuels

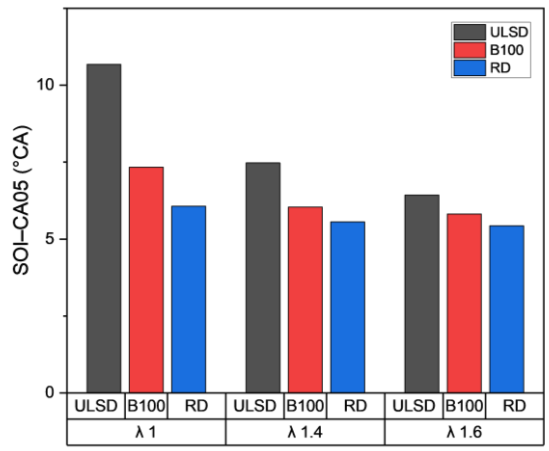

Figure 15. Ignition delay (SOI–CA05 duration) for all pilot fuels

4 CONCLUSIONS

A high-speed four-stroke diesel engine was operated at high NH_3 energy substitution levels with both petroleum diesel and biofuel pilot fuels. Key findings include:

1. Significant GHG reductions (~90%) are possible with high NH_3 energy substitution levels, even in high-speed diesel engines

2. Bio-pilot fuels can further reduce the lifecycle GHG contribution of CO_2 relative to petroleum diesel fuels
3. Renewable diesel and biodiesel were demonstrated to be suitable drop-in bio-pilots for dual-fuel ammonia without adverse performance on a four-stroke engine
4. Similar engine efficiency for NH_3 dual-fuel and diesel baseline with all pilot fuels; heat transfer is reduced, but fuel slip is significant.
5. N_2O is a significant contributor to the remaining GHG profile: engine-out N_2O emissions can be minimized at richer equivalence ratios; aftertreatment and net-negative bio-pilot fuels may further mitigate the impact.
6. NO and NH_3 emissions will require aftertreatment to mitigate
7. Black carbon emissions reduced for NH_3 dual-fuel combustion; further reductions from bio-pilots

5 DEFINITIONS, ACRONYMS, ABBREVIATIONS

°CA: crank angle degrees
λ: excess air ratio
ATDC: after top dead center
B100: 100% biodiesel fuel
BTDC: before top dead center
CA05: crank angle location of 5% mass fraction burned
CA50: crank angle location of 50% mass fraction burned
CI: compression-ignition
COV: coefficient of variability
FAME: fatty acid methyl ester
GHG: greenhouse gas
GWP: global warming potential
IMEP: indicated mean effective pressure
IMO: International Maritime Organization
IPCC: Intergovernmental Panel on Climate Change
ISCO: indicated specific emissions of carbon monoxide
$ISCO_2$: indicated specific emissions of carbon dioxide
ISHC: indicated specific emissions of unburned hydrocarbons
$ISNO_x$: indicated specific emissions of nitrogen oxides
ISN_2O: indicated specific emissions of nitrous oxide
ISPM: indicated specific emissions of particulate matter
PAH: polyaromatic hydrocarbons
RD: renewable diesel fuel
SI: spark-ignition
SOI: start of injection
TDC: top dead center
ULSD: ultra low sulfur diesel fuel

6 ACKNOWLEDGMENTS

This research was supported by the Department of Energy (DOE) Vehicle Technologies Office (VTO) and the Department of Transportation (DOT) Maritime Administration (MARAD). The authors would like to thank Kevin Stork and Gurpreet Singh at the DOE VTO and Galen Hon and Will Nabach at the DOT MARAD for their guidance and support.

The authors would also like to thank Cummins for supplying the engine used for this study and to acknowledge support from Steve Whitted, Scott Palko, Jonathan Willocks, and Vitaly Prikhodko at Oak Ridge National Laboratory.

7 REFERENCES

1. Valera-Medina A, Amer-Hatem F, Azad AK, Dedoussi IC, de Joannon M, Fernandes RX, *et al.* 2021. “Review on Ammonia as a Potential Fuel: From Synthesis to Economics,” *Energy & Fuels* 35(9): 6964–7029. doi:10.1021/acs.energyfuels.0c03685
2. International Maritime Organization (IMO). 2021. “2023 IMO Strategy on Reduction of GHG Emissions from Ships (MEPC 80 Annex 15)”
3. Alnajideen M, Shi H, Northrop W, Emberson D, Kane S, Czyzewski P, *et al.* 2024. “Ammonia Combustion and Emissions in Practical Applications: A Review,” *Carbon Neutrality* 3(13). doi:10.1007/s43979-024-00088-6
4. Forster P, Storelvmo T, Armour K, Collins W, Dufresne JL, Frame D, *et al.* 2021. “The Earth’s Energy Budget, Climate Feedbacks, and Climate Sensitivity,” in Masson-Delmotte V, Zhai P, Pirani A, Connors S, Péan C, Berger S, *et al.*, editors. *Climate Change 2021: The Physical Science Basis. Contribution of Working Group I to the Sixth Assessment Report of the Intergovernmental Panel on Climate Change*. Cambridge, UK and New York, NY, USA: Cambridge University Press; p. 923–1054. doi:10.1017/9781009157896.009
5. Mayer S, Kaltoft J, Christensen H, Cong S, Pang KM, Svensson J, *et al.* 2023. “Developing the MAN B&W Dual Fuel Ammonia Engine,” in *Proceedings of the 30th CIMAC World Congress,* Busan, Korea: Paper 589.
6. Schneiter D, Weber M, Goranov S. 2023. “Road to Zero Global Warming from High Powered Merchant Marine Propulsion Systems,” in *Proceedings of the 30th CIMAC World Congress,* Busan, Korea: Paper 454.

7. Portin K, Sariola L. 2023. “Safe and Efficient Engine Operation with Ammonia,” in *Proceedings of the 30th CIMAC World Congress,* Busan, Korea: Paper 231.

8. Wermuth N, Malin M, Schubert-Zallinger C, Engelmayer M, Wimmer A, Schlick H, *et al.* 2023. “Decarbonization of High-Power Systems: Ammonia-Hydrogen and Ammonia-Diesel Combustion in HS Engines,” in *Proceedings of the 30th CIMAC World Congress,* Busan, Korea: Paper 667.

9. Auer M, Kunkel C, Eppler F, Klaua T, Wilke I, Knafl A. 2023. “MAN Energy Solutions—Four-Stroke Engine Solutions for Low-Carbon and Carbon-Free Fuels,” in *Proceedings of the 30th CIMAC World Congress,* Busan, Korea: Paper 049.

10. Schlick H, Kammerdiener T, Murakami S, Carrasco MIS, Figer G, Malin M, *et al.* 2023. “Assessment of Combustion Concepts and Operational Limits of Net-Zero Carbon Fuels,” in *Proceedings of the 30th CIMAC World Congress,* Busan, Korea: Paper 105.

11. Niki Y, Hirata K, Kobayashi K, Shimizu Y. 2023. “Development of Premixed Ammonia Combustion Strategy with Minimum Emissions for Marine Diesel Engines,” in *Proceedings of the 30th CIMAC World Congress,* Busan, Korea: Paper 113.

12. Kurien C, Mounaim-Rousselle C. 2024. “Comparative Study on the Effect of Premixed Equivalence Ratio on Engine Characteristics of Ammonia Fuelled Engine Under Diesel Pilot Ignition vs Spark Ignition Combustion Mode,” in *Proceedings of the ASME 2024 ICE Forward Conference,* San Antonio, TX, USA: Paper No. ICEF2024-140740, V001T02A009. doi:10.1115/ICEF2024-140740

13. Jespersen MC, Rasmussen TØH, Ivarsson A. 2023. “Widening the Operation Limits of an SI Engine Running on Neat Ammonia,” in *Proceedings of the 30th CIMAC World Congress,* Busan, Korea: Paper 606.

14. Northrop WF. 2024. “Modeling Nitrogen Species from Ammonia Reciprocating Engine Combustion in Temperature-Equivalence Ratio Space,” *Applications in Energy and Combustion Science* 17(100245). doi:10.1016/j.jaecs.2023.100245

15. Kaul B, Kass M, Theiss T, Messner J, Tan E, Dutta A, *et al.* 2024. “Biofuels as Heavy Fuel Oil Substitutes in the Maritime Sector: Findings and Potential Pathways,” in *8th Rostock Large Engine Symposium 2024: The Future of Large Engines VIII: Technology Concepts and Clean Fuel Options: The Route to Clean Shipping,* Rostock, Germany. p. 1–15. doi:10.18453/rosdok_id00004632

16. Curran S, Kaul B. 2024. “Decarbonizing Shipping with Ammonia-Fueled Engines,” *EM Magazine*. November 2024.

17. Curran S, Onorati A, Payri R, Agarwal AK, Arcoumanis C, Bae C, *et al.* 2023. “The Future of Ship Engines: Renewable Fuels and Enabling Technologies for Decarbonization,” *International Journal of Engine Research* 25(1). doi:10.1177/14680874231187954

18. Curran SJ, Szybist JP, Wagner RM. 2012. “Reactivity Controlled Compression Ignition Performance with Renewable Fuels,” in *Proceedings of the ASME 2012 Internal Combustion Engine Division Fall Technical Conference,* p. 479–487. doi:10.1115/ICEF2012-92192

19. Karczewski M, Chojnowski J, Szamrej G. 2021. “A Review of Low-CO_2 Emission Fuels for a Dual-Fuel RCCI Engine,” Energies 14(16):5067. doi:10.3390/en14165067

20. Nadimi E, Przybyla G, Emberson D, Løvås T, Ziółkowski Ł, Adamczyk W. 2022. “Effects of Using Ammonia as a Primary Fuel on Engine Performance and Emissions in an Ammonia/Biodiesel Dual-Fuel CI Engine,” *International Journal of Energy Research*. doi:10.1002/er.8235

21. Qiu Y, Wei H, Zhou D, Zhou X, Li T. 2024. “Experimental Study on the Effect of Combustion and Emission Performance of Biodiesel-Ammonia Dual-Fuel Engine,” *Journal of Renewable and Sustainable Energy* 16(4): 043103. doi:10.1063/5.0208372

22. Xu H, Ou L, Li Y, Hawkins TR, Wang M. 2022. “Life Cycle Greenhouse Gas Emissions of Biodiesel and Renewable Diesel Production in the United States,” *Environmental Science & Technology* 56(12): 7512–7521. doi:10.1021/acs.est.2c00289

23. McCarney J. 2023. “Ammonia as a Fuel—A Role for Catalytic Components,” in *Proceedings of the 30th CIMAC World Congress,* Busan, Korea: Paper 440.

24. Curran S, Szybist J, Kaul B, Easter J, Sluder S. 2021. “Fuel Stratification Effects on Gasoline Compression Ignition with a Regular-Grade Gasoline on a Single-Cylinder Medium-Duty Diesel Engine at Low Load,” *SAE Technical Paper 2021-01-1173*. doi:10.4271/2021-01-1173.

25. Clean Air Power. “Clean Air Power Technologies,” [Online: cited 2025 March 4]. Available from: https://cleanairpower.com/technologies.

26. Dempsey A, Ghandhi J. 2016. “Engine Emissions & Uncertainty Analysis,” [Online: cited 2024 December 17]. Available from: http://sourceforge.net/projects/engine-emissions-uncertainty/files/.

27. Haltermann Solutions. “Ultra Low Sulfur 2007 Certification Diesel,” [Online: cited 2025 March 4]. Available from: https://www.haltermannsolutions.com/products?id=128414/ultra-low-sulfur-2007-certification-diesel

28. Tyrewala DS, Kaul BC, Curran SJ. 2025. “Experimental Investigation of Air-Fuel Equivalence Ratio Effects on Advanced Dual-Fuel Diesel/Ammonia Combustion on a Single-Cylinder Medium-Duty Diesel Engine at High Load,” in *Proceedings of the 14th U.S. National Combustion Meeting,* Boston, MA, USA.

29. Voniati G, Dimaratos A, Koltsakis G, Ntziachristos L. 2024. “Emission Control Concepts for Large Two-Stroke Ammonia Engines,” in *Proceedings of the 8th Rostock Large Engine Symposium,* Rostock, Germany. doi:10.18453/rosdok_id00004637

30. Patil T, Reggeti S, Kane SP, Northrop WF. 2024. “Experimental Investigation of Particulate Emissions from an Ammonia-Fueled Internal Combustion Engine,” in *Proceedings of the ASME 2024 ICE Forward Conference,* San Antonio, TX, USA: Paper No. ICEF2024-139956, V001T05A001. doi:10.1115/ICEF2024-139956

31. Mihai O, Tamm S, Stenfeldt M, Olsson L. 2016. “The Effect of Soot on Ammonium Nitrate Species and NO_2 Selective Catalytic Reduction over Cu-Zeolite Catalyst-Coated Particulate Filter,” *Philosophical Transactions of the Royal Society A.* 374(20150086). doi:10.1098/rsta.2015.0086

32. Smagala TG, Christensen E, Christison KM, Mohler RE, Gjersing E, McCormick RL. 2012. “Hydrocarbon Renewable and Synthetic Diesel Fuel Blendstocks: Composition and Properties,” *Energy & Fuels* 27(1): 237–246. doi:10.1021/ef3012849.

8 CONTACT

Brian Kaul
Senior Research & Development Staff
Oak Ridge National Laboratory
kaulbc@ornl.gov